The Role of Cohesion in Granular Fault Gouges on the Initiation of Sliding: Slip-Weakening Mechanisms and Energy Budget.

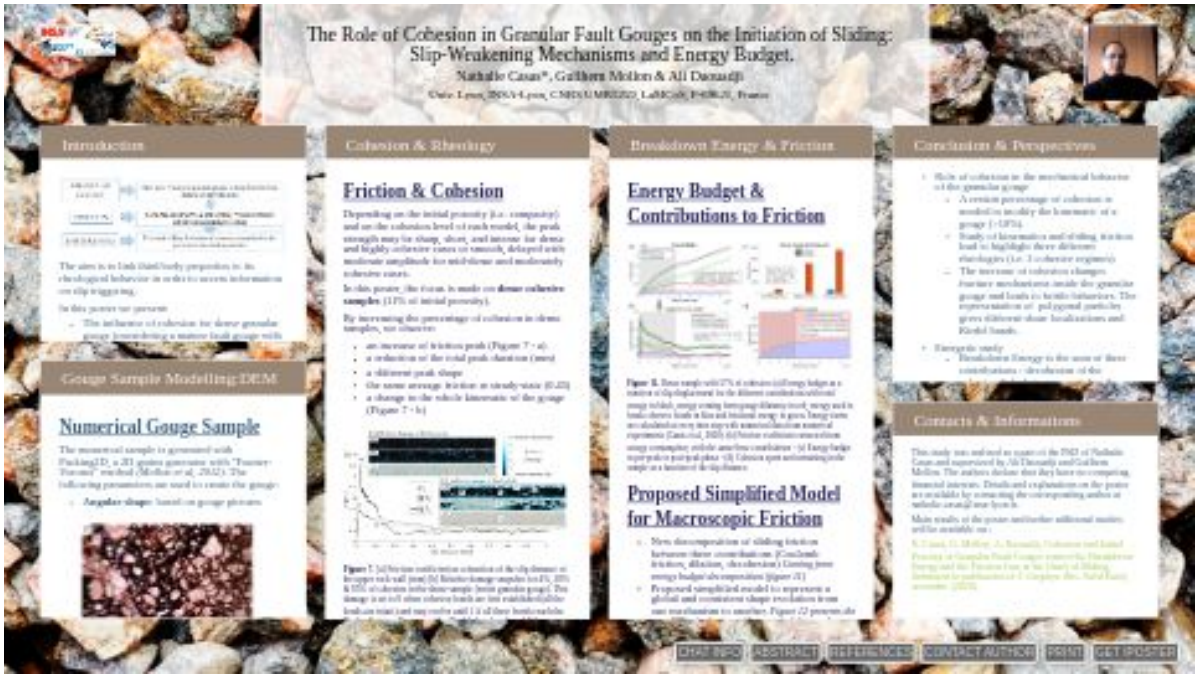

Nathalie Casas*, Guilhem Mollon & Ali Daouadji

Univ. Lyon, INSA-Lyon, CNRS UMR5259, LaMCoS, F-69621, France



PRESENTED AT:

INTRODUCTION

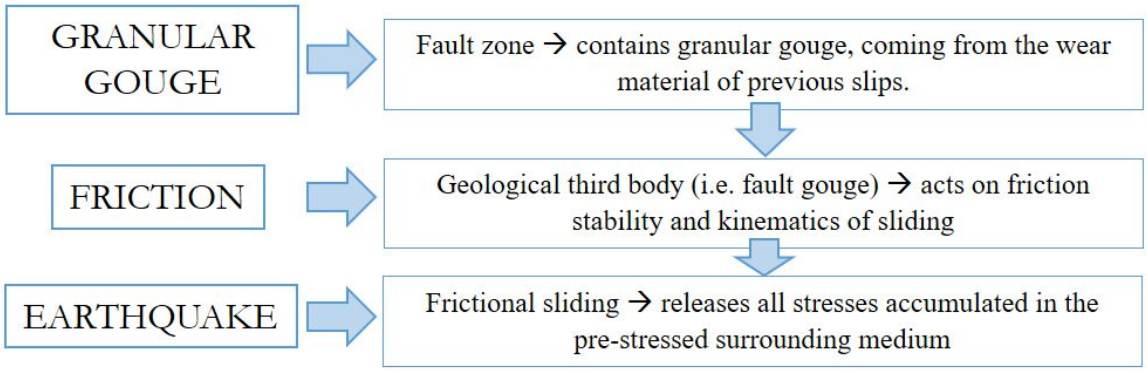

The aim is to link third body properties to its rheological behavior in order to access information on slip triggering.

In this poster we present:

- The influence of cohesion for dense granular gouge (considering a mature fault gouge with mineral cementation between particles).
- The observation of Riedel shear bands formation with two different granular samples.
- A partitioning of macroscopic friction and Breakdown Energy into three main contributions: dilation, decohesion and Coulomb friction. And a comparison to classical slip-weakening mechanisms

We chose to use Discrete Element Method.

GOUGE SAMPLE MODELLING:DEM

Numerical Gouge Sample

The numerical sample is generated with Packing2D, a 2D grains generator with "Fourier-Voronoï" method *(Mollon et al, 2012)*. The following parameters are used to create the gouge:

- **Angular shape**: based on gouge pictures

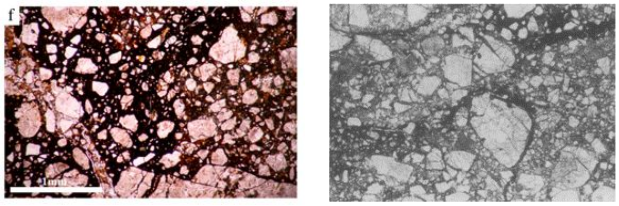

Figure 1. Images from (Muto et al., 2015), (Blenkinsop, 1991) with granular and faceted grain shape

- **Fractal distribution** (D=2.6): 4960 particles with an equivalent diameter in the range 28 – 260 µm. *(Olgaard & Brace, 1983), (Blenkinsop, 1991), (Billi & Storti, 2004), (Muto et al., 2015)*
- Representative Surface Element: **2x20mm²**. Zoom in on generated grains sample:

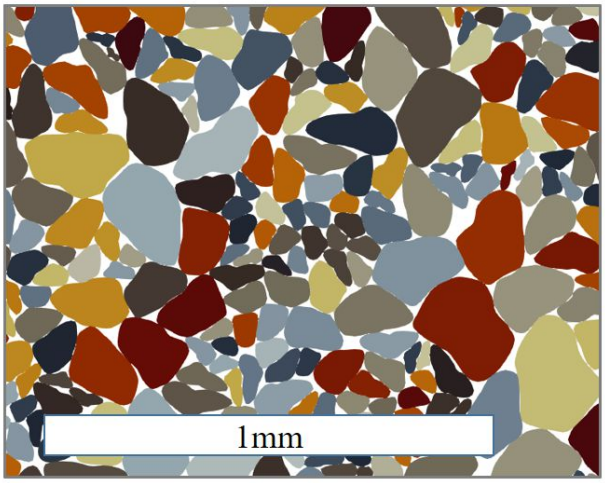

Figure 2. Grains sample generated with Packing2D (Mollon et al, 2012). Angular shape and fractal distribution (D=2.6).

Direct Shear Experiment with DEM

- **Discrete Element Method** has already shown its ability to represent granular gouges with relevant kinematics and rheology. *(Morgan & Boettcher, 1999), (Da Cruz et al., 2005)*

We use the software **MELODY 2D** by (Mollon, 2016):

Discretized Element Method = DEM

DEM →

- To compute motions of a large number of particles
- Every particle is considered as a body with dynamic equations
- Interactions with other bodies

MELODY = Multibody ELement-free Open code for DYnamic simulation (Mollon, 2016)

Allows to represent in the same digital frame the 1st and 3rd bodies with their deformation and dynamics:

- to keep the discontinuity of the 3rd body → Multi-body
- to take into account the inertial and damping effect → Dynamic

Figure 3. Advantages of DEM and MELODY, the software is freely available here (http://guilhem.mollon.free.fr/).

- **Dry cohesive** contact model in 2D (Figure 4).

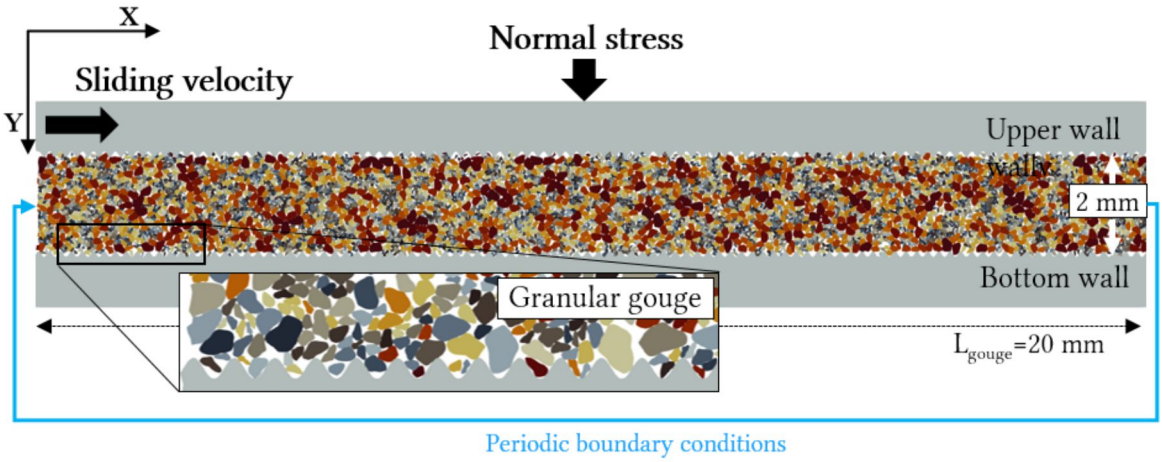

Figure 4. DEM model of a granular fault gouge, 4960 angular particles in a 2x20mm domain. Granular gouge between two rough rock walls, normal stress of 40 MPa and sliding velocity of 1m/s applied on the upper rock wall. Periodic boundary conditions at both sides of the model (right to left). Volumetric mass of 2600 kg/m^3.

Cohesive Contact Law

The mineral cementation within a mature fault gouge is simulated by cohesive links between particles.

- **Contact interactions**

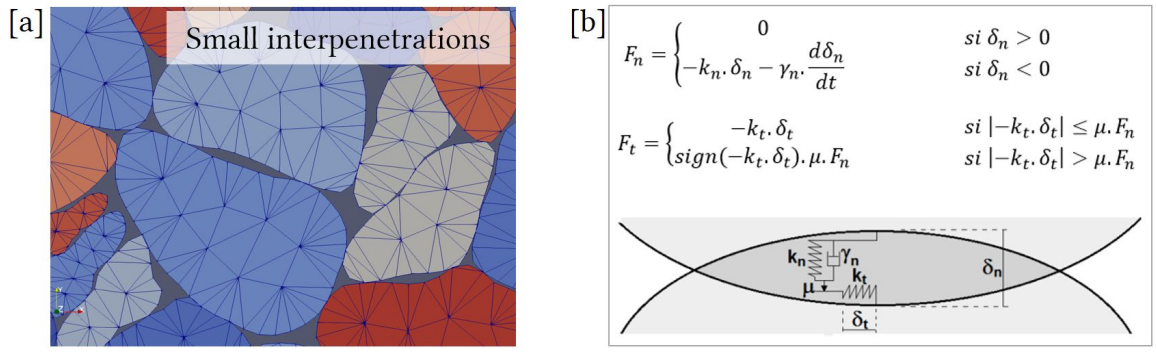

Rigid grains → High numerical stiffness

Optimized proximity and contact detection → 3 steps of contact detection

Figure 5. [a] Each grain contour is discretized by nodes and segments. Contacts considered are between a node from one grain and a segment from another grain. [b] Computation of a normal gap δn (obtained by projecting the node on the segment) and a tangential gap δt (integrated in time based on the history of the relative motions of the node and the segment in the tangential direction). Used to compute contact forces F_n & F_t, more detailed in (Mollon, 2018). k_n & k_t represent normal and tangential stiffnesses, μ the friction.

- **Cohesive contact law**

Typical contact life for cohesive law (Figure 6):

- The bond corresponds to a pressure C_n maintaining particles in contact (Pa).
- Two possible status (intact or broken)
- Once broken, a contact cannot be cohesive again and this induces an increase of broken bonds during the shearing.

The cohesion presented in next results is normalized with respect to a representative Energy, and expressed as a percentage of cohesion X% within the model (more detailed in (Casas et al., 2020)).

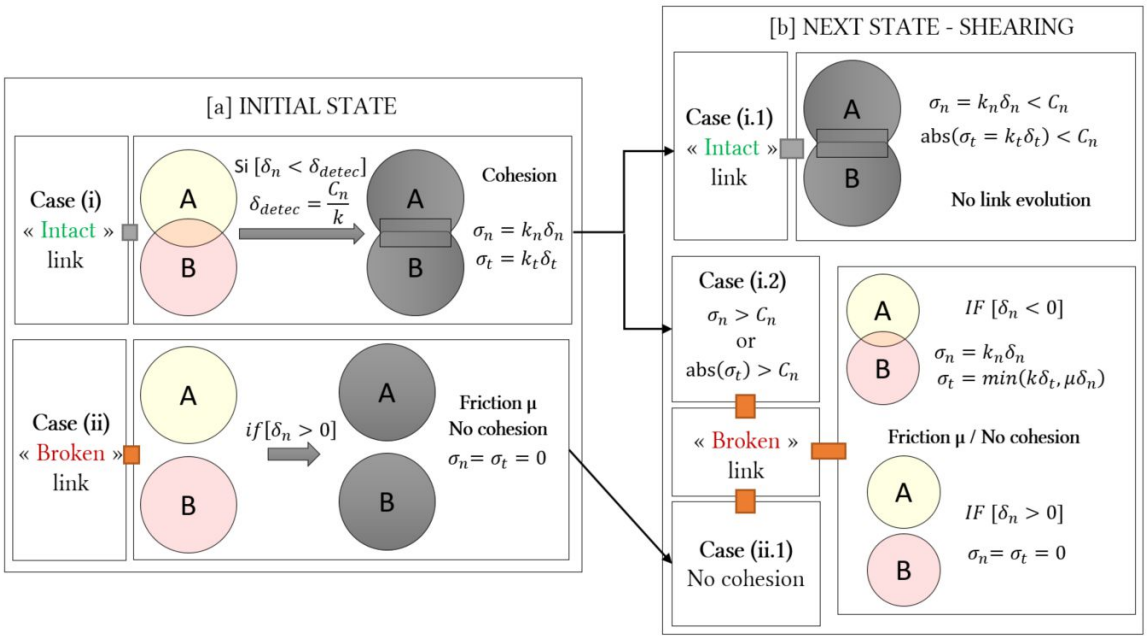

Figure 6. From left to right. [a] Initial state with two status: (i) intact if grains are initially in contact (interpenetration between grains) or (ii) broken is there is an initial gap between grains (δn>0). This step depends on the numerical cohesion C_n applied between grains and on the numerical stiffness k. Normal and tangential stresses can also be computed, σn and σt. [b] Next state, with shearing of the gouge: (i.1) the cohesive contact can still be intact, no evolution, or, (i.2) grains can be in contact, but with no cohesion anymore or, (ii.2) grains can be far enough to not consider a contact (no contact forces).

COHESION & RHEOLOGY

Friction & Cohesion

Depending on the initial porosity (i.e. compacity) and on the cohesion level of each model, the peak strength may be sharp, short, and intense for dense and highly cohesive cases or smooth, delayed with moderate amplitude for mid-dense and moderately cohesive cases.

In this poster, the focus is made on **dense cohesive samples** (11% of initial porosity).

By increasing the percentage of cohesion in dense samples, we observe:

- an increase of friction peak (Figure 7 - a)
- a reduction of the total peak duration (mm)
- a different peak shape
- the same average friction at steady-state (0.45)
- a change in the whole kinematic of the gouge (Figure 7 - b)

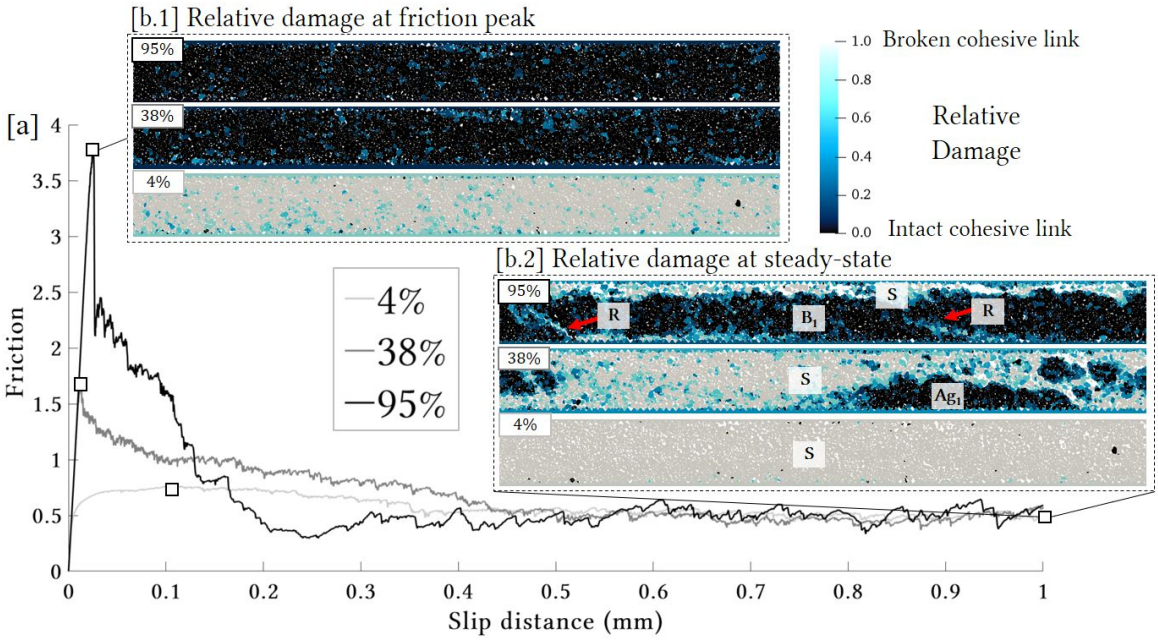

Figure 7. [a] Friction coefficient as a function of the slip distance of the upper rock wall (mm) [b] Relative damage snapshot for 4%, 38% & 95% of cohesion in the dense sample (entire granular gouge). This damage is set to 0 when cohesive bonds are first established (all the bonds are intact) and may evolve until 1 if all these bonds reach the “broken” status. R represent the Riedel shear bands and S the horizontal shear localization.

Gouge thickness and solid fraction within the gouge:

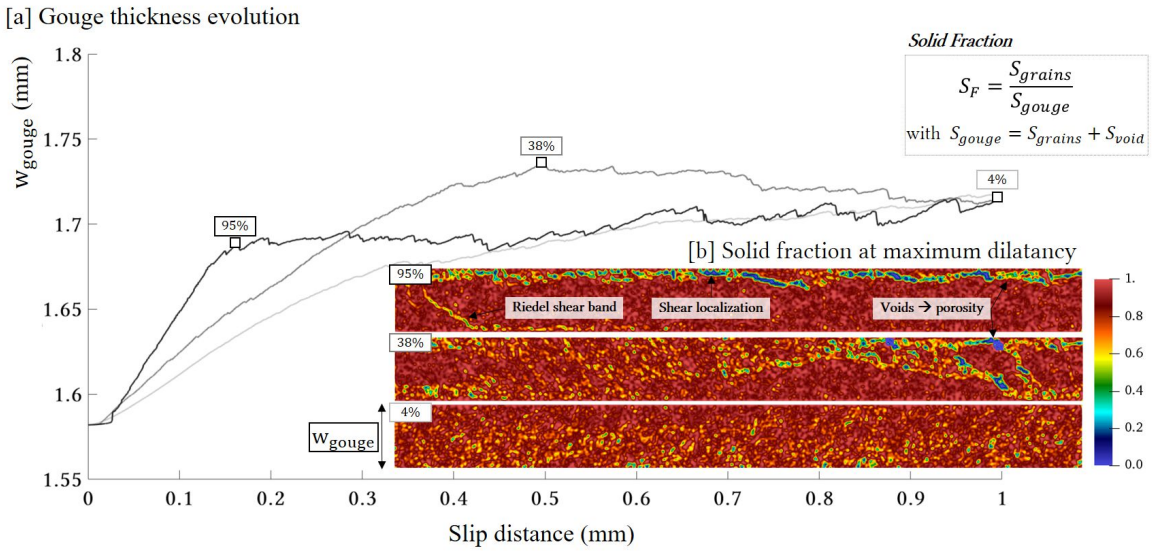

Figure 8. [a] Gouge thickness evolution (mm) as a function of the slip distance (mm) for 4%, 38% & 95% of cohesion – [b] Solid fraction at the maximum dilatancy observed in the three samples, presence of Riedel bands and shear localization.

Rheology & Kinematics

3 types of cohesive regimes highlighted with different failure patterns (Riedel cracks, shear bands, etc.):

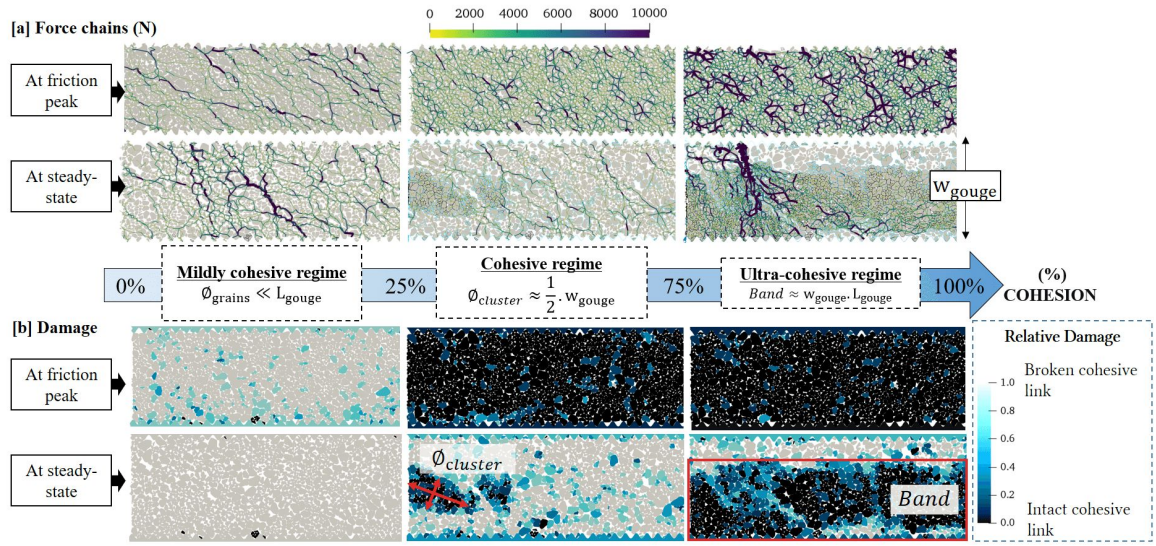

Figure 9. [a] Force chains as a function of the percentage of cohesion, at friction peak and at steady state. Three regimes of cohesion. [b] Relative damage snapshot for 4%, 38% & 95% of cohesion for dense samples. This damage is set to 0 when cohesive bonds are first established (all the bonds are intact) and may evolve until 1 if all these bonds reach the "broken" status.

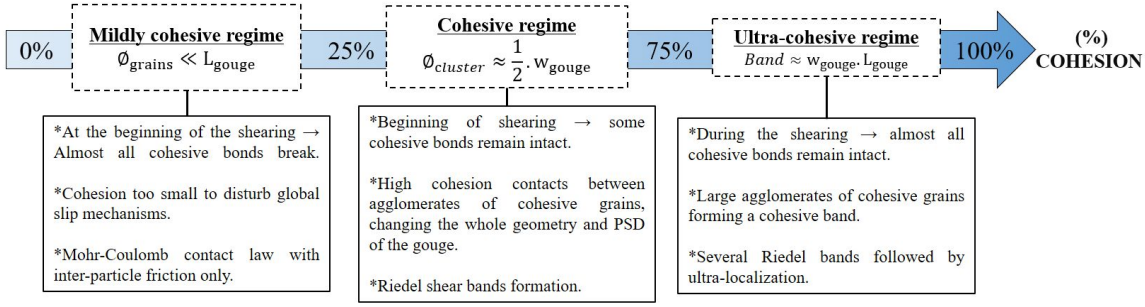

These regimes also correspond to an evolution of the amount of ductility within the sample.

- A very dense or highly cohesive sample behaves as a brittle material
- A typical cohesionless and porous geological layer tends to behave as a ductile material.

Initial porosity inside the sample changes packing of particles, and thus the application of cohesion. Shear bands do not follow the same patterns for mid-dense samples (see paper of (Casas et al., 2020)).

Relative damage evolution between mildly cohesive and cohesive regime:

[VIDEO] https://www.youtube.com/embed/4Gb0q9T-weY?rel=0&fs=1&modestbranding=1&rel=0&showinfo=0

Movie 1. Comparison of the evolution of relative damage with slip distance for dense samples (entire granular gouge 2x20mm²), between 8% cohesion (mildly cohesive regime) and 38% cohesion (cohesive regime). From zero imposed slip to the beginning of steady state.

Relative damage evolution between cohesive and ultra-cohesive regime:

[VIDEO] https://www.youtube.com/embed/-SiBgnM2KUA?rel=0&fs=1&modestbranding=1&rel=0&showinfo=0

Movie 2. Comparison of the evolution of relative damage with slip distance for dense samples (entire granular gouge 2x20mm²), between 38% cohesion (cohesive regime) and 95% cohesion (ultra-cohesive regime). From zero imposed slip to the beginning of steady state.

Matrix vs Cohesion ?

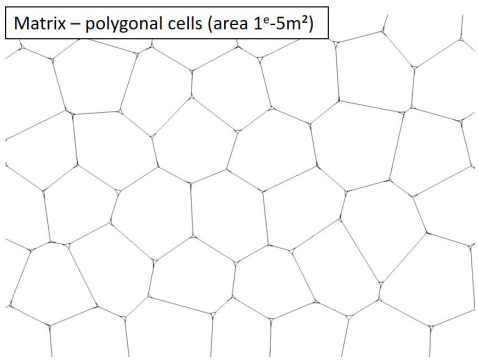

New gouge sample with Polygonal cells (i.e. 0.01% porosity) and Coulomb friction law (no cohesion)

- New failure patterns: Riedel shear bands very pronounced compared to previous results with Angular grains (i.e. 11% initial porosity) + cohesive law (Figure 10)
- Emergence of Riedel bands before friction peak for polygonal cells, in contrast with angular grains
- *Next step: a mixture of angular grains and matrix (representing cementation between grains as cohesion prevously studied)*

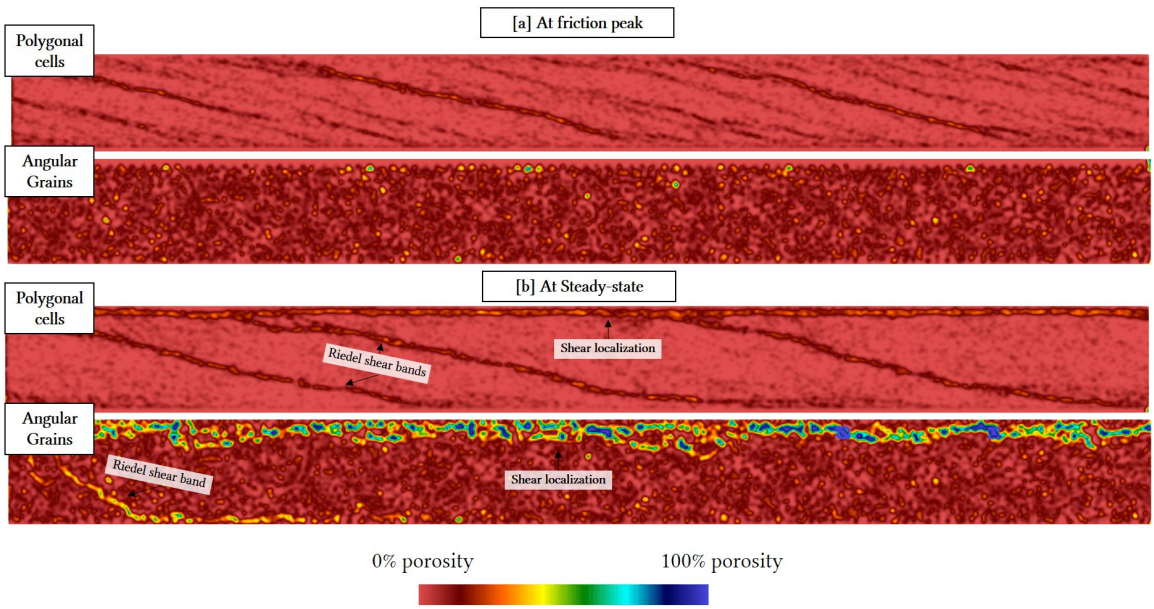

Figure 10. Fracture patterns in dense third body layers as a function of the percentage of porosity within the sample for angular grains (i.e. 11% initial porosity) and polygonal cells (i.e. 0.01% porosity) – [a] Friction peak [b] Steady-state

[VIDEO] https://www.youtube.com/embed/Z9EBNrdq0ZY?rel=0&fs=1&modestbranding=1&rel=0&showinfo=0

Movie 3. Evolution of solid fraction with slip distance for a sample with polygonal cells (i.e. 0.01% porosity). From zero imposed slip to steady state.

BREAKDOWN ENERGY & FRICTION

Energy Budget & Contributions to Friction

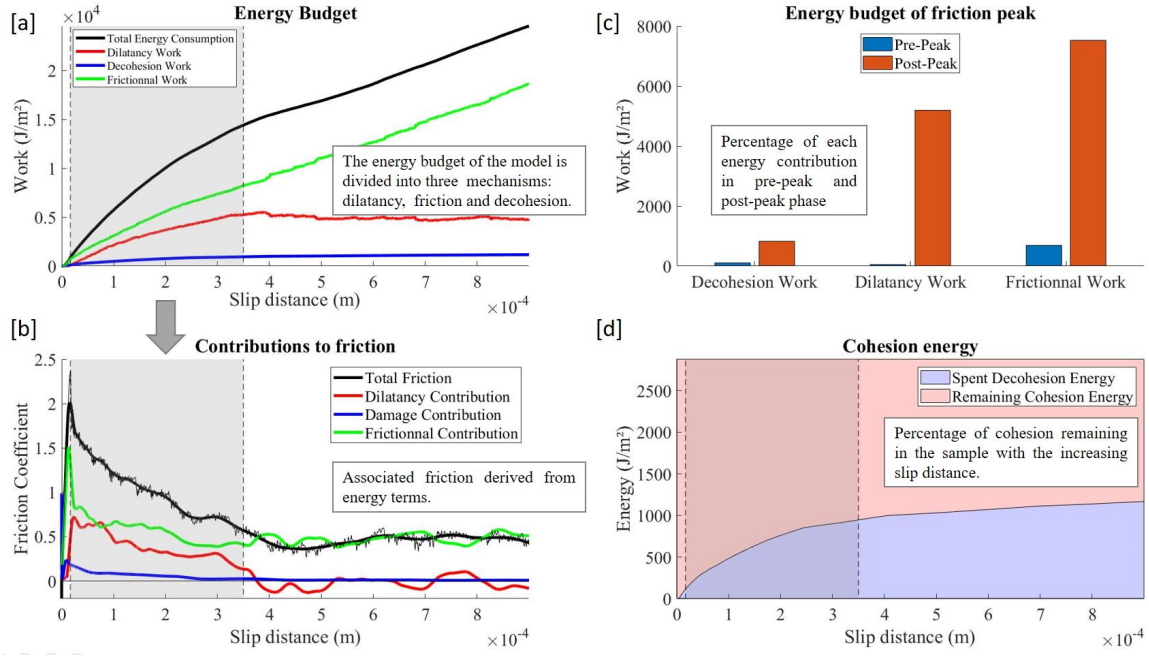

Figure 11. Dense sample with 57% of cohesion: (a) Energy budget as a function of slip displacement for the different contributions with total energy in black, energy coming from gouge dilatancy in red, energy used to break cohesive bonds in blue and frictional energy in green. Energy terms are calculated at every time step with numerical data from numerical experiments (Casas et al., 2020). (b) Friction coefficient extracted from energy consumption, with the same three contributions - (c) Energy budget in pre-peak or post-peak phase - (d) Cohesion spent and remaining in the sample as a function of the slip distance.

Proposed Simplified Model for Macroscopic Friction

- New decomposition of sliding friction between three contributions (Coulomb friction, dilation, decohesion) *Coming from energy budget decomposition (figure 11)*
- Proposed simplified model to represent a global and consistent shape evolution from one mechanism to another. *Figure 12 presents the case 38% of cohesion with numerical data and simplified models.*

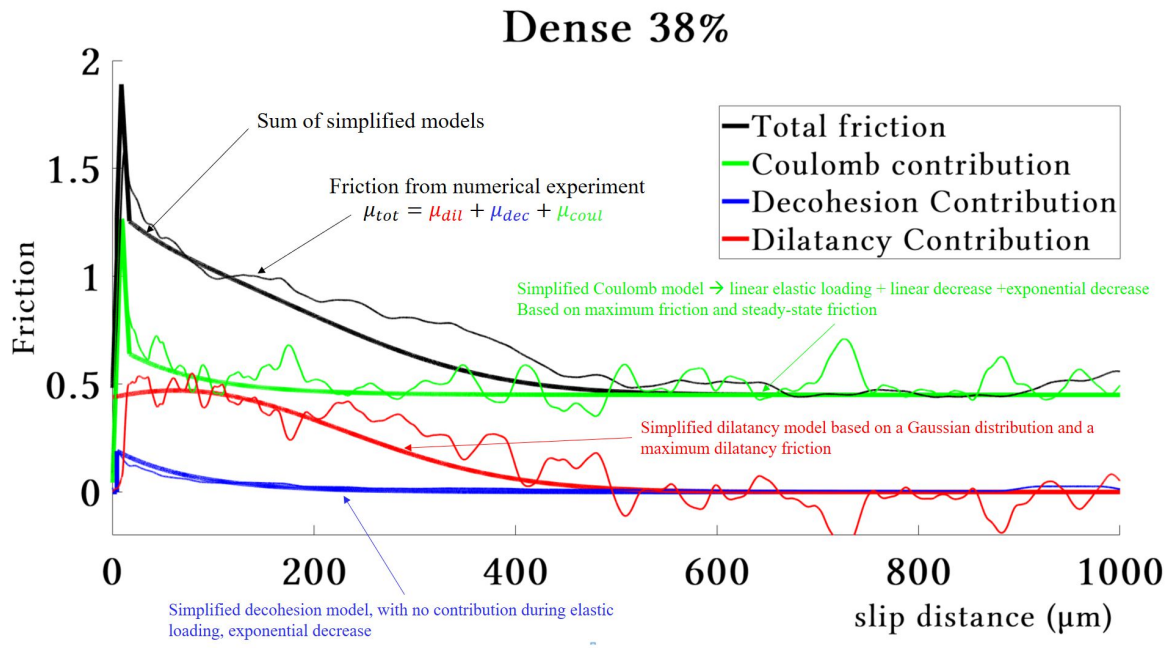

Figure 12. Friction-slip curve with different contributions (dilatancy in red, Coulomb in green and decohesion in blue) - dense sample – 38% of cohesion – The black curve is the sum of all contributions. Bold lines represent the proposed simplified model and thin curves the numerical results.

Details on the model are available in (Casas et al., 2020).

- Direct link between rheology and physics

Opportunity to identify when and where (on the onset of sliding.) the different mechanisms are acting. *Figure 13 displays the simplified models obtained for different values of cohesion, dense samples.*

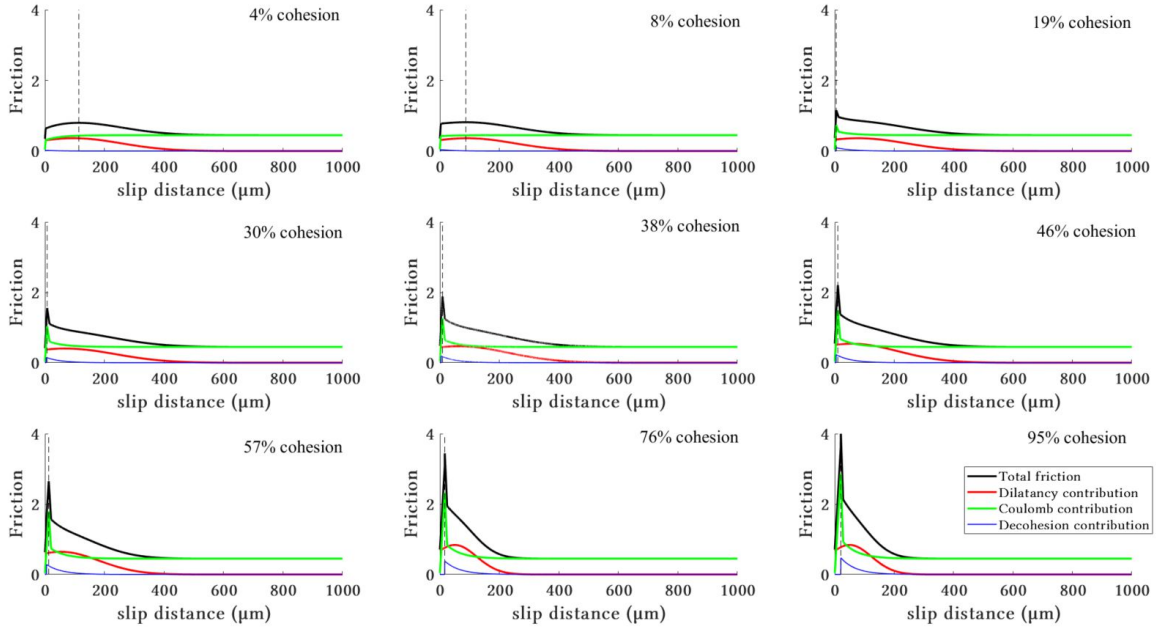

Figure 13. Proposed simplified models - Evolution of friction contributions as a function of the slip distance, for different percentage of cohesion. Dense sample - Mildly cohesive regimes with a diminution of the pre-peak phase with the increase of cohesion (0% to 25%) – Cohesive regimes with a negligible pre-peak phase but an important influence of friction peak (25% to 75%) – Ultra cohesive regimes with almost not pre-peak phase and an very high Coulomb friction peak (75% to 100%).

Breakdown Energy

- During an earthquake, energy is dissipated during fault sliding by means of different mechanisms, theoretical model based on slip-weakening theory. *In (Figure 14-a), based on [(Kanamori & Heaton, 2000), (Abercrombie & Rice, 2005)].*
- The local Breakdown energy = energy needed to weaken the fault can be divided into 3 energy contributions terms (heating processes are not taking into account) Calculated with the proposed schema, and compared to classical energy budget theory (Figure 14– b).

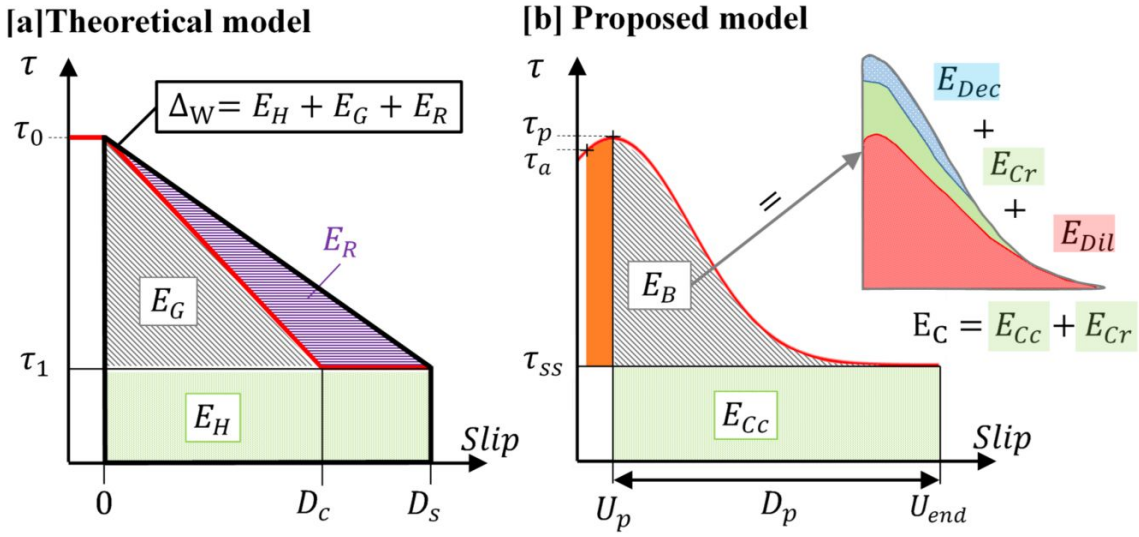

Figure 14: (a) Theoretical model of energy budget ΔW as the sum of a fracture energy E_G, a radiated energy E_R (propagating by the mean of elastic waves) and a frictional energy E_H (dissipated within the slip zone). τ_0 is the initial static shear stress, $\tau_1$the dynamic shear stress, D_C is the slip

weakening distance and D_S the end of slip displacement. This energy budget model is based on linear slip weakening theory - (b) Proposed model (function shape strongly varies depending on cohesion and compaction), with decomposition of the breakdown energy E_B. E_B gathers a dilatancy energy E_{dil} linked to sample dilation (mechanical energy), a Decohesion energy E_{dec} coming from the breakage of cohesive links (surface creation energy) and E_{Cr} a part of Coulomb energy E_C. is the initial static shear stress, is the maximum shear stress, is the steady-state shear stress, or dynamic shear stress. D_P is the friction peak duration. Coulomb energy E_{Cr} collects all the Coulomb energy that is not considered in the constant part E_{Cc}.

- Dilation appears to be the most influent factor *(Figure 15)*
- Pre-peak Breakdown Energy need to be considered in mildly cohesive regime *(Figure 13) and (Figure 15)*

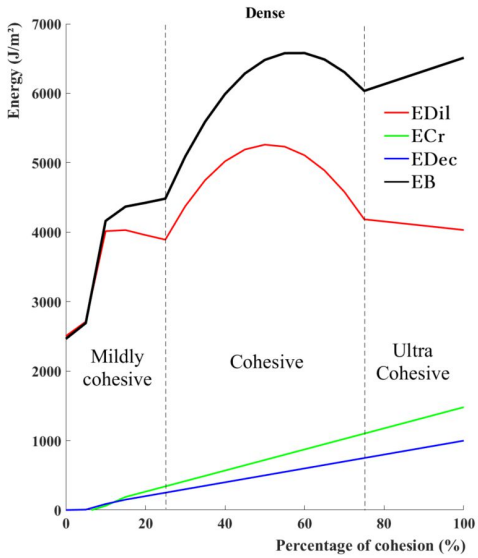

Figure 15. Breakdown energy (J/m²) coming from the different contributions as a function of the percentage of cohesion within the gouge for dense samples. E_B (in black) gathers a dilatancy energy E_{dil} (in red) linked to sample dilation (mechanical energy), a Decohesion energy E_{Dec} (in blue) coming from the breakage of cohesive links (surface creation energy) and E_{Cr} (in green), a part of Coulomb energy E_C.

Our slip weakening models for friction:

- can fit with a wide range of experiment, and give a different decreasing slope in comparison to classical linear or exponential SW models.
- can be adapted to others stresses and slip velocity
- could be implemented in dynamic rupture modelling at higher scales

CONCLUSION & PERSPECTIVES

- Role of cohesion in the mechanical behavior of the granular gouge
  - A certain percentage of cohesion is needed to modify the kinematic of a gouge (>10%).
  - Study of kinematics and sliding friction lead to highlight three different rheologies (i.e. 3 cohesive regimes).
  - The increase of cohesion changes fracture mechanisms inside the granular gouge and leads to brittle behaviors. The representation of polygonal particles gives different shear localizations and Riedel bands.
- Energetic study
  - Breakdown Energy is the sum of three contributions : decohesion of the cohesive links between particles, the dilatancy of the gouge and frictional contacts.
  - Pre-peak Breakdown energy cannot be neglected for mildly cohesive regime (i.e. <25% cohesion).
  - The proposed simplified models can be implemented in dynamic studies at larger scales.

Perspectives

- To create a new sample as a mixture between angular grains AND mineral matrix between grains, and to study shear bands evolution.

CONTACTS & INFORMATIONS

This study was realized as a part of the PhD of Nathalie Casas and supervized by Ali Daouadji and Guilhem Mollon. The authors declare that they have no competing financial interests. Details and explanations on the poster are available by contacting the corresponding author at nathalie.casas@insa-lyon.fr.

Main results of the poster and further additional studies will be available on :

N. Casas, G. Mollon, A. Daouadji, Cohesion and Initial Porosity of Granular Fault Gouges control the Breakdown Energy and the Friction Law at the Onset of Sliding, *Submitted to publication in J. Geophys. Res. Solid Earth, november (2020).* (https://www.essoar.org/doi/abs/10.1002/essoar.10504966.1)

ABSTRACT

Fault zone usually presents a granular gouge, coming from the wear material of previous slips. Considering a mature fault gouge with mineral cementation between particles, we aim to understand the influence of these cohesive links on slip mechanisms. As cohesion is difficult to follow and to quantify with Lab or in-situ experiments, we choose to use Discrete Element Method that has already shown its ability to represent granular gouges with relevant kinematics and rheology. In this work, we consider a dry cohesive contact model in 2D (2x20mm²) involving two rough surfaces representing the rock walls separated by the granular gouge (5000 particles, grain size 27- 260 µm). A step forward compared to literature is to add cohesion on real angular and faceted grains that modifies contact between particles. Focusing on physics of contacts inside the granular gouge, we explore contact interactions and friction coefficient between the different bodies. To represent the cementation we set up a Bonded Mohr-Coulomb law, considering that inter-particular bridges and particles are made with the same material. This numerical model is displacement-driven and is implemented to study the peak of static friction (shape, slope, duration) under a confined pressure of 40 MPa. Depending on the compacity and on the cohesion level of each model, the peak strength may be sharp, short, and intense for dense and highly cohesive cases or smooth, delayed with moderate amplitude for mid-dense and moderately cohesive cases. Three main behaviors are observed: a non-cohesive regime where the added cohesion is too small to truly disturb the global slip mechanism (Couette flow), an intermediate cohesive regime with clusters of cohesive grains changing the granular flow and acting on slip weakening mechanisms (Riedel shear band R1) and an ultra-cohesive regime where gouge behaves as a brittle material with several Riedel shear bands emergence. We also investigate the role of cohesive bonds in energy budget, focusing on fracture energy term. Three mechanisms are playing a role in fracture energy evolution: the rupture of cohesive bonds, the dilatancy of the gouge and Coulomb dissipations due to friction. These factors are linked to the initial percentage of cohesion inside the sample and help characterize the mechanisms at stake in the initiation of sliding.

REFERENCES

[1] G. Mollon, J. Zhao, Fourier-Voronoi-based generation of realistic samples for discrete modelling of granular materials, Granul. Matter. (2012) 621–638. https://doi.org/10.1007/s10035-012-0356-x.

[2] J. Muto, T. Nakatani, O. Nishikawa, H. Nagahama, Fractal particle size distribution of pulverized fault rocks as a function of distance from the fault core, Geophys. Res. Lett. 42 (2015) 3811–3819. https://doi.org/10.1002/2015GL064026.

[3] T.G. Blenkinsop, Cataclasis and Processes of Particle Size Reduction, Pure Appl. Geophys. 136 (1991) 59–86.

[4] D.L. Olgaard, W.F. Brace, The microstructure of gouge from a mining-induced seismic shear zone, Int. J. Rock Mech. Min. Sci. Geomech. 20 (1983) 11–19. https://doi.org/10.1016/0148-9062(83)91610-8.

[5] A. Billi, F. Storti, Fractal distribution of particle size in carbonate cataclastic rocks from the core of a regional strike-slip fault zone, Tectonophysics. 384 (2004) 115–128. https://doi.org/10.1016/j.tecto.2004.03.015.

[6]J.K. Morgan, M.S. Boettcher, Numerical simulations of granular shear zones using the distinct element method: 1. Shear zone kinematics and the micromechanics of localization, J. Geophys. Res. Solid Earth. 104 (1999) 2703–2719. https://doi.org/10.1029/1998jb900056.

[7]F. Da Cruz, S. Emam, M. Prochnow, J.N. Roux, F. Chevoir, Rheophysics of dense granular materials: Discrete simulation of plane shear flows, Phys. Rev. E. 72 (2005) 1–17. https://doi.org/10.1103/PhysRevE.72.021309.

[8] G. Mollon, A multibody meshfree strategy for the simulation of highly deformable granular materials, Int. J. Numer. Methods Eng. 108 (2016) 1477–1497. https://doi.org/10.1002/nme.5258.

[9] G. Mollon, A unified numerical framework for rigid and compliant granular materials, Comput. Part. Mech. 5 (2018) 517–527. https://doi.org/10.1007/s40571-018-0187-6.

[10] N. Casas, G. Mollon, A. Daouadji, Cohesion and Initial Porosity of Granular Fault Gouges control the Breakdown Energy and the Friction Law at the Onset of Sliding, Submitted to J. Geophys. Res. Solid Earth in november 2020.

[11] H. Kanamori, T.H. Heaton, Microscopic and Macroscopic Physics of Earthquakes, in: J.B. Rundle, D.L. Turcotte, W. Klein (Eds.), Geocomplexity Phys. Earthquakes, 2000: pp. 147–163. https://doi.org/10.1029/GM120p0147.

[12] R.E. Abercrombie, J.R. Rice, Can observations of earthquake scaling constrain slip weakening ?, Geophys. J. Int. 162 (2005) 406–424. https://doi.org/10.1111/j.1365-246X.2005.02579.x.